Assessing the Positional Uncertainties of Geometric Corrected Remote Sensing Images

Carlos Antonio Oliveira Vieira, *UFV Viçosa*
Giuliano Sant'Anna Marotta, *UFV Viçosa*
Dalto Domingos Rodrigues, *UFV Viçosa*
Rafael Andrade, *UFV Viçosa*

Conteúdo [esconder]

1. Introduction

High spatial resolution of orbital sensors provides greater facility on the collection of control points to perform the geometric correction of remote sensing images. However, it is important to be careful and precise during the process of obtain these reference coordinates, because inherent errors to the reference coordinates, as well as the processes of obtain them, can propagate uncertainty to derived products. Therefore, in order to evaluate the quality of these geometrically corrected images, there is a need to involve techniques that put in evidence the positional uncertainty on explicit and spatial form.

Thus, the objective of this article is to evaluate and to visualize uncertainties that occur through the geometric correction process of remote sensing images and its effect into the final coordinates of geometrically corrected images. Moreover, it is also noticed that knowing the positional coordinates, and its uncertainties, allows the analyst to determine the potentialities and applications of the geometrically corrected image, related to the positional aspect.

2. Material and Methods

2.1 Study Area

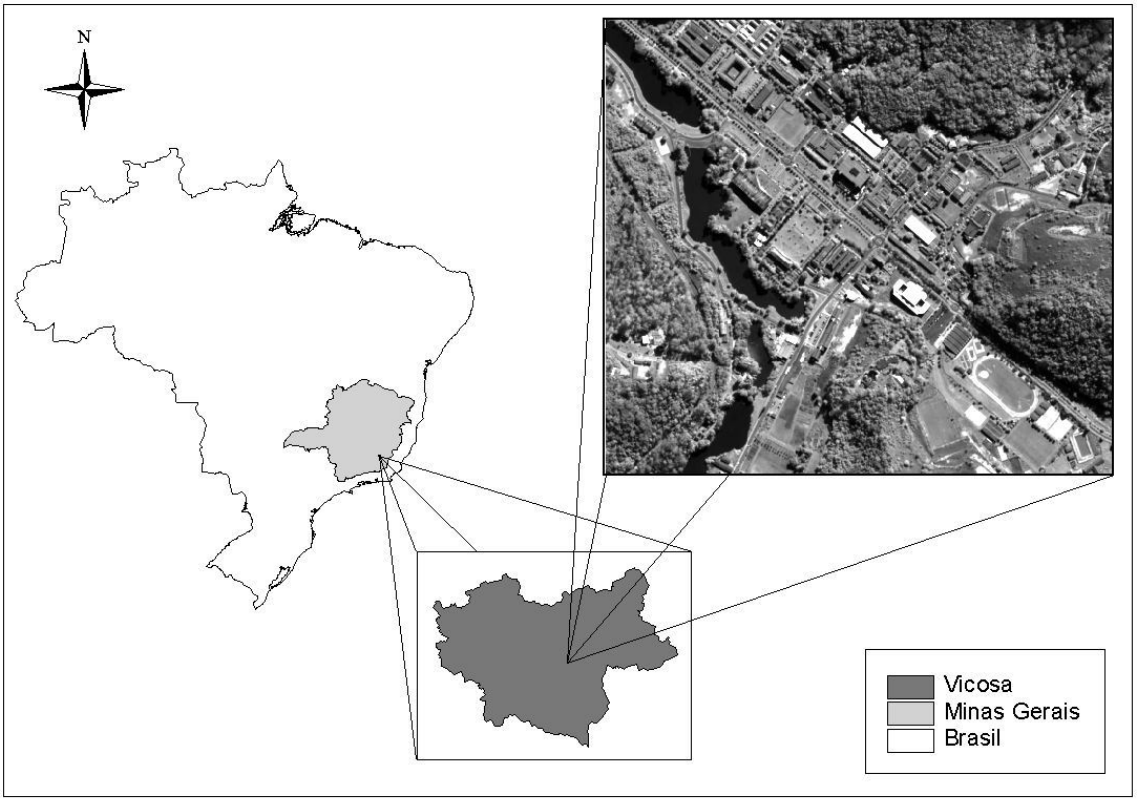

Fig. 1 : Study area location and a sample of the Quickbird image used

The study area is located in the southeast of Brazil, on the Minas Gerais State, at the Campus of the Federal University of Viçosa (Figure 1). The region has a dramatic landscape, with mountains all over the region.

2.2 Material

It was used a QuickBird image in order to carry out the experiments, with spatial and radiometric resolution of 0.60m and 11 bits respectively. It was also used the system ERDAS Imagine 8.3.1 version, for visual control points extractions and visualizations.

Three Ashtech Promark II GPS receivers were used to collect Ground Control Points (GCP) and the Trimble Geomatics Office 1.63 software was also used to process and adjust the coordinates.

It was collected 13 very well defined and distributed ground control points and their homologous ones on the Quickbird image. Figure 2 shows the ground control points and their location in relation to the VICO GPS reference station, which belongs to the *Brazilian Geodesic Network of Continuous Monitoring* (RBMC).

2.3 Methods

The firs step was an identification of control features, and then perform the extraction of the coordinates in a Quickbird image and the determination of their homologous reference coordinates on the ground, using a GPS Receiver (Arruda, 2002).

A topographical polygon was implanted on the field, with many vertices. This polygon was linked to three known GPS points of the Brazilian National Grid, covering 1,5 km square inside the study area at the campus of the Federal University of Viçosa.

The polygon computation was carried out using the parametric model of the *Least Mean Squares* (LMS) method that provided the positional covariance for every polygon vertices (i.e., GCP). This process allowed to get know, the positional uncertainties associates to all the used GCP, which is needed to perform the orbital image geometric correction (Baltsavis et al., 2001).

Using the reference coordinates and their homologous image extracted coordinates were calculated the transformation parameters, using two different transformation models: affine and projective ones and their variants for two dimensions (2D) and three dimension (3D) transformations. Such procedure allows the association of a positional uncertainty of the image corrected as a function of the inherent uncertainties from the reference coordinates. In addition, these uncertainties had been propagated through the transformation parameters to the rectified image coordinates.

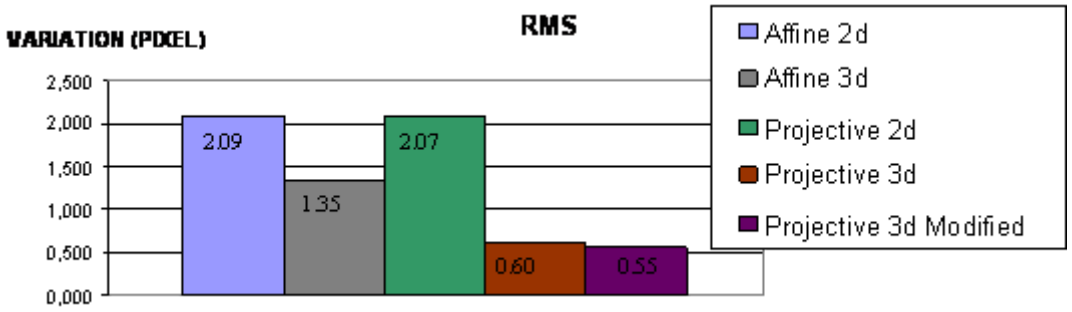

Fig. 2 : Ground Control Points (GCP) and VICO RBMC Station

Transformations models are mathematical equations used to transform coordinates between projection systems. The affine and projective transformations models and their variants will be presented in the following sub-sections.

2.3.1 The Affine Models

The affine model for 2D uses six parameters to model transformations between projections systems (Fraser 2004). These parameters are: two translation parameters (?C, ?L); one rotation parameter (k), two scale factors (?u, ?v) and a factor of non-orthogonally between axes (?xy), which are presented in the following equations:

$$C = \lambda u.X.\cos k - \lambda v.Y.\mathrm{sen}k + \Delta C \qquad (1)$$

$$L = \lambda u.X.\text{sen}(k + \varepsilon xy) + \lambda v.Y.\cos(k + \varepsilon xy) + \Delta L \quad (2)$$

where X and Y are the reference coordinates and C (column) and L (line) are their homologue image coordinates.

The affine model can be written using a matrices notation:

$$\begin{bmatrix} C \\ L \end{bmatrix} = \begin{bmatrix} a_1 & a_2 \\ a_4 & a_5 \end{bmatrix} \cdot \begin{bmatrix} X \\ Y \end{bmatrix} + \begin{bmatrix} a_3 \\ a_6 \end{bmatrix} \quad (3)$$

Thus, in order to perform the 2D transformations model it is necessary to have at least the coordinates of three points on the image and their homologues on the ground (references). However, it is necessary to have redundant observations in order to perform the parametric LSM method and have an idea of the observation quality and estimated parameters (Pedro, 2003).

According to Lugnani (1987) the affine model projects the 3D space to the 2D, which is the particular case of the central projection, where the projections point was dislocated to infinite. The affine model for 3D can be extended to:

$$\begin{bmatrix} C \\ L \\ z \end{bmatrix} = \begin{bmatrix} a_1 & a_2 & a_3 \\ a_5 & a_6 & a_7 \\ a_9 & a_{10} & a_{11} \end{bmatrix} \cdot \begin{bmatrix} X \\ Y \\ Z \end{bmatrix} + \begin{bmatrix} a_4 \\ a_8 \\ a_{12} \end{bmatrix} \quad (4)$$

where onde : C, L, z – represent the point coordinates on the image space; and X, Y, Z – represent the point coordinates on the object space; and, $a_1 ... a_{12}$ – represent the transformation parameters.

2.3.2 The Projective Models

The projective models represent a simplification of the co-linearity model (Mitishita et al., 2003). According to Andrade (2003) a bi-dimensional projective coordinate transformation requires eight parameters and the utilization of this transformation model is appropriated when a bi-dimensional coordinate system is projected to other one that is no parallel. Summing up, the projective model includes non parallelism between the Cartesian systems.

It is necessary to not consider the altitude of the points on the object space ($Z_P = 0$), and after the inherent simplifications of the original projective model, the following equations are derived for the 2D projective model:

$$C = \frac{a_1 X + a_2 Y + a_3}{a_7 X + a_8 Y + 1} \quad (5)$$

$$L = \frac{a_4 X + a_5 Y + a_6}{a_7 X + a_8 Y + 1} \quad (6)$$

where: C, L – represent the point coordinates on the image space (C_p, L_p); X,Y – represent the point coordinates on the object space (X_p, Y_p); a_1...a_8 – represent the transformation parameters.

Similarly, the 3D projective transformation model also performs inherent simplifications on the original projective model, however, this model considers the altitude value (Z_p ? 0) in order to determine the parameters and on the coordinate transformation between non orthogonal systems, as follow:

$$C = \frac{a_1X + a_2Y + a_3Z + a_4}{a_9X + a_{10}Y + a_{11}Z + 1} \quad (7)$$

$$L = \frac{a_5X + a_6Y + a_7Z + a_8}{a_9X + a_{10}Y + a_{11}Z + 1} \quad (8)$$

where: C, L – represent the point coordinates on the image space (Cp, Lp); X, Y, Z – represent the point coordinates on the object space (X_p, Y_p, Z_p); a_1...a_{11} – represent the transformation parameters.

There is also an alternative modified model, named by Wang (1999) and Valadan (2003) as *Calibration Direct Linear Transformation* (SDLT), which consists in an addition of one more parameter (a_{12}) on the Equation (8), referring to the 3D projective model. This 3D modified projective model defines 14 parameters that promote the relation between the 2D and 3D space, as following:

$$C = \frac{a_1X + a_2Y + a_3Z + a_4}{a_9X + a_{10}Y + a_{11}Z + 1} \quad (9)$$

$$L = \frac{a_5X + a_6Y + a_7Z + a_8}{a_9X + a_{10}Y + a_{11}Z + 1} + a_{12}CL \quad (10)$$

According to Wang (1999) this 3D modified projective model represents a linear transformation process between image and ground coordinates, with an additional correction for the image coordinates (parameter), in order do adjust systematic errors. Using this model, there is no need for the use of interior orientation parameters, neither for use of approximated exterior orientation parameters (ephemerid information).

The determination of these parameters, for all these transformations models, used the parametric *Least Mean Square* (LMS).

2.3.3 Parameters' Determination

The determination of these parameters, for all these transformations models, used the parametric *Least Mean Square* (LMS) method, in which the observations (L_b) plus the observation residuals (V) must be equal to the function F(X_a) of the mathematical model used (Gemael, 1994), in relation to adjusted parameters:

$$L_b + V = F(X_a) \quad (11)$$

A stochastic model was set up based on variances of the screen coordinates observed (C_{Lb}). These variances were arbitrary chosen and all of them had the same standard deviations, as following:

$$C_{Lb} = \mathrm{diag}\,[\ \sigma_{C_1}^2\ \ \sigma_{L_1}^2\ \ ..\ \ \sigma_{C_N}^2\ \ \sigma_{L_N}^2\ ] \quad (12)$$

This arbitrary procedure of have chosen the variances *a priori* is utilized for the computations of the weights on the observations, which is recomputed due to a variance in the *a posteriori* adjustment, in order to adequate to the adjusted parameters.

After the computation of parameters and weight fitness, it is computed the variance-covariance matrix (VCM) of the observed values and of the adjusted parameters, which is generated by:

$$C_{PAR} = \hat{\sigma}_0^2 . (A^t . P . A)^{-1} \quad (13)$$

Using these adjusted parameters and the extracted image coordinates (C and L), it is possible perform the transformation between systems through the inverse model and obtain the coordinates (X, Y and Z) for every pixel of the image in the geodesic system.

2.3.4 Models Evaluations and Positional Error Map Generation

The precision of the adjustment model was performed using both: the RMS error analysis and the verification of the *a posteriori sigma 0*, which was evaluated through the X^2 statistical test, using a significance level of 0.05, for each transformation model. Thus, to perform these computations, it is necessary to multiply the *a posteriori* reference variance by the freedom degree and compare it with the tabled value. If the computed value is inside of a tabled interval, the assumed hypothesis is accepted, in which the *a priori* reference variance is statistically equal to the *a posteriori* reference variance.

In order to compute the *a posteriori* adjustment variance uses the equations:

$$\hat{\sigma}_0^2 = \frac{V^t . P . V}{GL} \quad (14)$$

$$P = \sigma_0^2 . C_{Lb}^{-1} \quad (15)$$

where P is the observations residuals and GL is the freedom degree (the difference between the number of observations and the number of parameters).

After the acceptance of the precision test, the uncertainties of the transformation parameters and of the reference coordinates were propagated into the geometrically corrected image, and then, RMS errors were generated for every pixel in the image. Thus, a *positional error map* could be generated, using the individual RMS, in meters, for each pixel of the image.

3. Results

Table 1 presents the set of 13 coordinates, which were collected directly from the satellite image. It is observed that the collection error for each coordinate was assumed to be 0.5 pixels for every collected point and the altitudes were not collected.

Points	C (pixel)	C error (pixel)	L (pixel)	L error (pixel)	h (pixel)	h error (pixel)
1	708	0.500	1324	0.500	0	0.000
2	278	0.500	184	0.500	0	0.000
3	1719	0.500	1600	0.500	0	0.000
4	335	0.500	867	0.500	0	0.000
5	1043	0.500	879	0.500	0	0.000
6	1462	0.500	1278	0.500	0	0.000
7	690	0.500	568	0.500	0	0.000
8	1227	0.500	207	0.500	0	0.000
9	1723	0.500	354	0.500	0	0.000
10	1446	0.500	510	0.500	0	0.000
11	369	0.500	1627	0.500	0	0.000
12	1587	0.500	871	0.500	0	0.000
13	1083	0.500	1378	0.500	0	0.000

In addition, it was performed a field collection of homologous points, identified from the image, using GPS receivers. The data were processed using the RBMC VICO as reference GPS station, and results are presented on the Table 2.

The next step was to perform the observations adjustment using the *Least Mean Square* method for each transformation model and then it was evaluated the precision of every model through the RMS error and the verification of the *a posteriori sigma 0* analysis (Marotta and Vieira, 2005).

Points	X (m)	X error (m)	Y (m)	Y error (m)	h (m)	h error (m)

1	721833.861	0.001	7702378.716	0.001	650.998	0.002
2	721585.024	0.001	7703060.306	0.001	647.328	0.003
3	722441.781	0.001	7702224.542	0.001	656.256	0.003
4	721614.844	0.001	7702652.644	0.001	647.328	0.003
5	722039.943	0.002	7702650.328	0.001	654.516	0.004
6	722289.909	0.001	7702415.010	0.001	656.254	0.002
7	721829.400	0.000	7702834.126	0.000	651.286	0.001
8	722154.039	0.001	7703049.621	0.001	709.544	0.002
9	722451.907	0.009	7702966.922	0.004	677.397	0.023
10	722283.740	0.002	7702872.384	0.002	665.209	0.005
11	721630.932	0.079	7702198.404	0.018	661.354	0.073
12	722366.429	0.001	7702656.512	0.001	695.651	0.003
13	722060.586	0.001	7702350.609	0.001	691.864	0.004

The global RMS error for each transformation model is presented in Figure 3. It is shown that the best RMS error was obtained by the 3D projective modified model (0.55 pixels) and the worst one was obtained by the 2D affine model (2.09 pixels), as expected. The 3D projective model presented very similar RMS error (0.60 pixels). These results point out the importance of choose a better transformation model in order to perform the geometric corrections in remote sensed data.

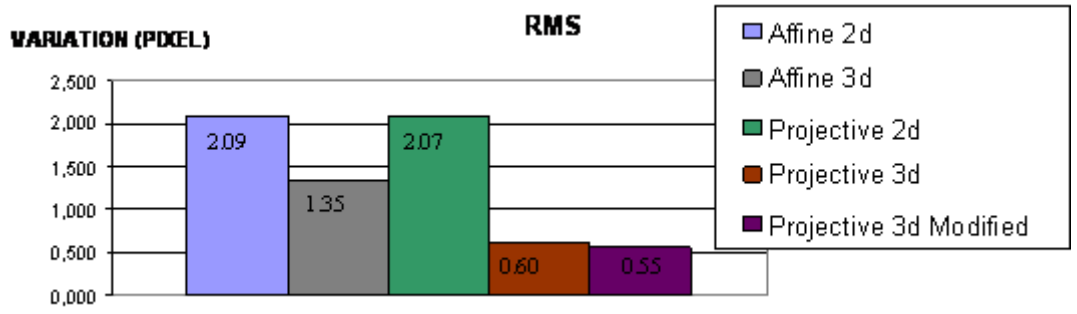

Fig. 3 : The RMS error behaviours for each transformation model using LMS adjustment

Figure 4 show a graph with the *a posteriori* variances behavior for each transformation model after the LMS adjustment. The results were very consistent with the RMS error analysis. Observing the results, it is possible to conclude that both the 3D projective and the 3D

projective modified models obtained the best adjustment results, compared to the other ones. Moreover, it is observed that both models presented very similar values too.

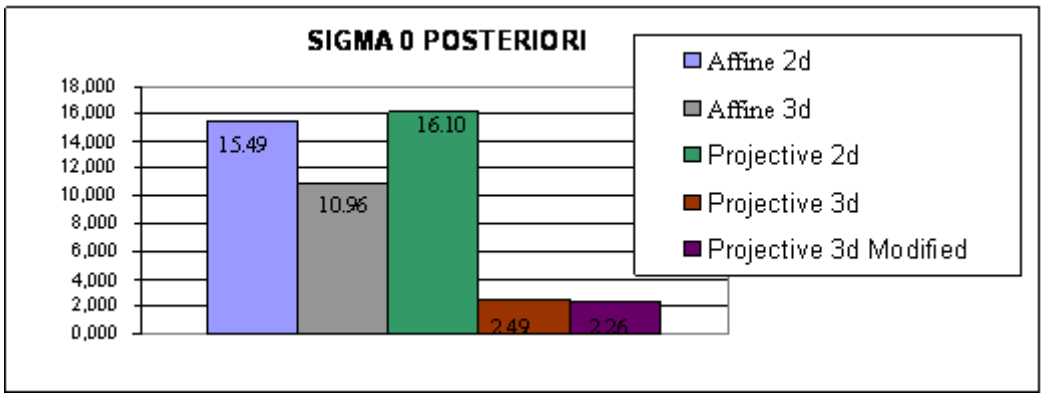

Fig. 4 : *A posteriori* variances behaviour for each transformation model using LMS adjustment

Although these measures indicate the best and the worst transformation model to be used, they are non spatial statistic measures; therefore, they do not consider the positional aspect of the uncertainty. In order to perform a spatial evaluation of uncertainty it was proposed a method, in which is performed variances propagation through the inverse transformation models to obtain the RMS errors, from residual, for every image pixel, bring adjusted parameters uncertainty into the transformed coordinates.

Figure 5 presents a *positional error map* for each transformation model. Thus, after the spatialization uncertainty process, it is possible to evaluate areas where the positional accuracy is less precise than other one. The analyst could consider the possibility of densification of control points in this area in order to improve the positional accuracy and a better adjustment of the transformation model.

Although the non spatial statistic measures (RMS error and sigma *a posteriori*) point out the 3D projective modified model as the best one, through the propagation of the uncertainty, it is possible to conclude that the 3D projective model presented a better result.

4. Conclusion

After perform the experiments, it is conclude that the best RMS error was obtained by the 3D projective modified model and the worst one was obtained by the 2D affine model. The 3D projective model and 3D projective modified one were very similar in performance. These results point out the importance in choose a better transformation model in order to perform the geometric corrections in remote sensed data. In addition results show that the uncertainties increases as pixels get far away from the support polygon (i.e., GCP), which emphasize the importance of select a number of GCP spread all over the study area. Moreover, using the proposed *positional error map*, it is possible to evaluate every observation, with its precisions, offering high confidence in the transformed image coordinates. It is also important to mention that the use of the variance propagation rules allows analyzing the residual uncertainties of the transformation parameters spatially in the entire image. Research needs to be developed in order to verify the potential use of these tools for uncertainties visualization of geometrically corrected remote sensing images. Considering the *positional error map* the 3D projective model presented a better transformation result.

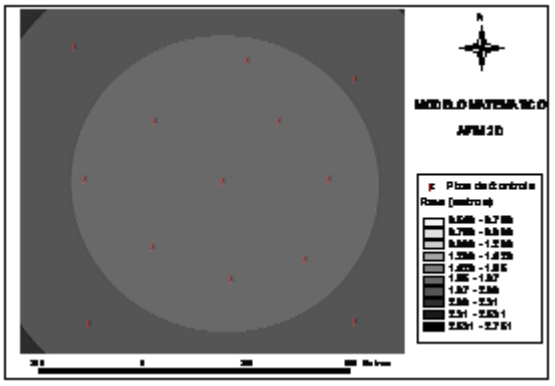

Fig. 5a : Affine 2D

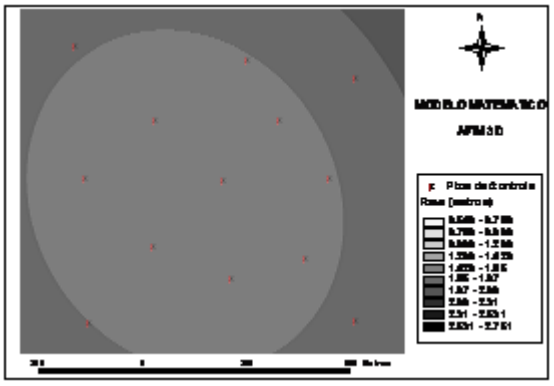

Fig. 5b : Affine 3D

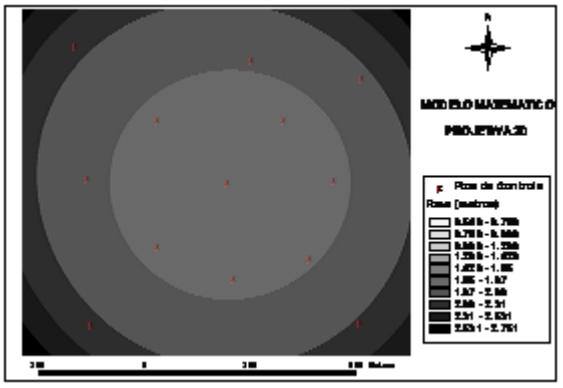

Fig. 5c : Projective 2D

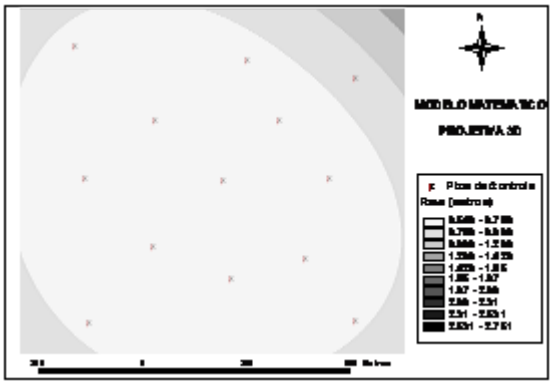

Fig. 5d : Projective 3D

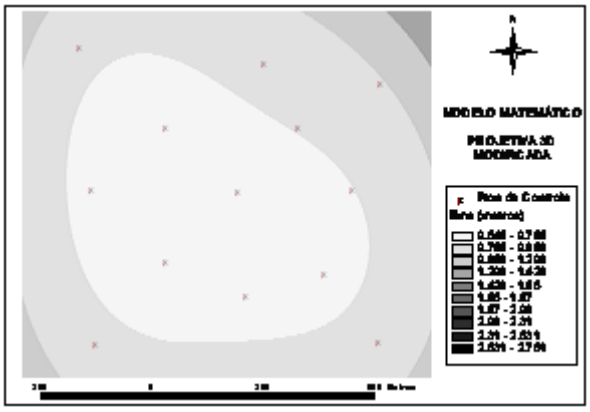

Fig. 5a : Projective 3D Modified

Fig. 5: The spacialisation of the errors for each transformation model.

5. Acknowledgements

Research by Mr. Marotta and Mr. Andrade were supported by the Brazilian Research Council (Capes) performed in collaboration with Civil Engineering Post-Graduation Program (UFV). We are grateful to PSA Research Group for permission to use their images. We would like to

thanks the Civil Engineering Department and Surveying Engineering Sector for the use of their equipments and softwares.

6. References

1. **Andrade,J.B.:** ***Fotogrametria*****, 2ª Edição. Curitiba – PR, SBRR Press, UFPR, 2003**
2. **Arruda jr.,E.R.:** ***Mosaicagem de imagens digitais*****, MSc Dissertation – FCT/UNESP, 2002**
3. **Baltsavias,E.; Pateraki,M.; Zhang,L.: Radiometric and Geometric Evaluation of Ikonos Geo Images and Their Use for 3d Building Modelling. Hannover – Germany,** ***ISPRS Workshop "High Resolution Mapping From Space*****, pp. 19-21, 2001**
4. **Fraser,C.S.; Amakawa,Y.: Insights into the affine model for hight-resolution satellite sensor orientation..** ***Journal of Photogrammetry & Remote Sensing*** **– ISPRS, 58, pp. 275-288, 2004**
5. **Gemael,C.:** ***Introdução ao ajustamento de observações: aplicações geodésicas geodésicas*****. Curitiba – PR, Universidade Federal do Paraná - UFPR, 319p., 1994**
6. **Lugnani,J.B.:** ***Introdução à Fotogrametria*****. Curitiba – PR, Universidade Federal do Paraná – UFPR, 134p., 1987**
7. **Marotta,G.S.; Vieira,C.A.O.: Aplicação do Padrão de Exatidão Cartográfica em Imagens Orbitais Aster Para Fins de Atualizações de Mapeamentos. In:** ***XXII Congresso Brasileiro de Cartografia*****, Macaé – RJ, 2005**
8. **Mitishita,E.A.; Saraiva,C.C.S.; Machado,A.L.: Monorrestituição de Imagens do Satélite De Alta Resolução Ikonos 2 (Geo), Utilizando-Se da Transformação DLT e Modelo Digital de Terreno., In:** ***XI Simpósio Brasileiro de Sensoriamento Remoto*****, p. 357-364, Belo Horizonte – MG, 2003**
9. **Pedro,P.C.:** ***Ortorretificação de Imagens de Alta Resolução Ikonos E Quickbird Utilizando O Modelo Apm (Affine Projection Model)*****, Dissertação de Mestrado em Ciências Geodésicas – UFPR, Curitiba – PR, p. 97, 2005**
10. **Valadan Zoej,M.J.; Sadeghian,S.:** ***Rigorous and Non-Rigorous Photogrammetric Processing of Ikonos Geo Image*****. Disponível em 10/07/2007: http://www.ipi.uni-hannover.de/html/publikationen/2003/workshop/valadan.pdf**
11. **Wang,Y.: Automated triangulation of linear scanner imagery. In:** ***Veröffentlichungen des Instituts für Photogrammetrie und Ingenieurvermessungen*****, Joint Workshop of ISPRS WG I/1, I/3 and IV/4, 18,** ***Sensors and Mapping from Space*****, Hanover, September 27-30, 1999**